# Effect of pixel active area shapes on microscanning based infrared super-resolution imaging

Sun Mingjie, Yu Kanglong

(Institution of Opto-electrionics Technology, Beihang University, Beijing 100191, China)

**Abstract:** Super-resolution (SR) imaging is a technology based on oversampling to reduce the aliasing and increase the image resolution. Pixel active area (PAA) model is essential in SR related research. The difference of MTF with the widely used square model and the "Z" shape model we proposed was calculated to simulate the practical infrared focal plane array (IRFPA) production. The cause of the difference was analyzed. Furthermore, a hypothesis was proposed, which the smaller the difference between the closest and the farthest distances from the PAA boundaries to the pixel center, the greater the MTF of IRFPA will be. Different PAA shapes were discussed and the MTFs of these shapes were calculated. The calculation results verify the hypothesis we proposed. These results also show that the circle PAA is the most ideal model and it should be used as a reference for IR FPA design.

**Key words:** microscanning; infrared super-resolution imaging; pixel active area shape

**CLC**: TP911.73 **Document code**: A **Article ID**: 1007-2276(2015)01-0048-05

# 像素有效形状对微扫描红外超分辨成像的影响

孙鸣捷,于康龙

(北京航空航天大学 仪器科学与光电工程学院,北京 100091)

**摘 要**:超分辨成像是基于过采样来降低频率混叠、提高图像分辨率的技术,而像素有效形状是超分辨相关研究的重要对象。基于实际的红外焦平面阵型提出了"Z"形有效形状模型,并分析了常用的方形模型和"Z"形模型分别得到调制传递函数(MTF)的差别。还提出了形状边界到中心点的差值越小,其得到的 MTF 越大的假设,通过对不同形状模型的 MTF 推导分析和数值模拟,其结果证实了这一假设。数值模拟结果还表明圆形模型具有最大的 MTF 值。上述结论对未来的红外焦平面阵型设计与生产具有参考意义。

**关键词**:微扫描; 红外超分辨成像; 像素有效形状

**收稿日期**:2014-05-07; **修订日期**:2014-06-10

**基金项目**:国家自然科学青年基金(61307021)

**作者简介**:孙鸣捷(1982-),男,博士,主要从事光电成像方面的研究。Email:09559@buaa.edu.cn

## 0 Introduction

Infrared focal plane array (IRFPA) imaging has been developed rapidly for two decades and is widely used. However, the IRFPA pixel pitch, the distance between the centers of adjacent pixels, is not small enough, so the captured images will be degenerated due to frequency aliasing. Super-resolution (SR) imaging is a technology based on oversampling to reduce the aliasing and increase the image resolution[1-3]. It provides an innovative, cost-effective system for IR imaging.

A proper mathematical model of image degeneration is essential to super-resolution imaging[4]. Since Hock, for the first time [5], discussed effect of oversampling in pixel array based on the assumption that the pixel active area (PAA) shape was a square model (shown in Fig.1(a)), such assumption is widely cited in the later research of SR imaging [6-13]. However, the PAA shapes of most IRFPA productions are actually not ideal square, for example, in Fig.1(b), the micrograph of a real IRFPA production shows that its PAA is a "Z" kind shape. It is important to simulate and calculate the difference between the MTF of the real PAA and that of the ideal square PAA.

On the other hand, although the real PAAs are not strictly square due to the production techonology, they are intentionally designed to be a square. In another word, the square model becomes a standard reference for IRFPA design. However, the square model hasn't been verified as the most ideal model, which would degenerate the image quality the least.

Therefore, hereinafter is to discuss the MTF difference between the real PAA and the ideal square, and what kind of shape is the most ideal model.

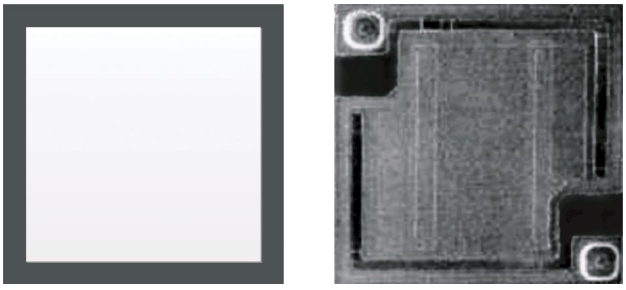

(a)　(b)

Fig. 1 (a) Square PAA of an ideal FPA, (b) PAA of GW20020131A GWIC Inc. (China)

## 1 Quantitative assessment of real IRFPA production

Modulation transfer function (MTF) is used for imaging system evaluation, the lower MTF value means the larger image degeneration. The following research is based on the analysis of MTF with different PAA shapes. In order to simulate the pixel of a real IRFPA production in Fig.1(b), a "Z" shape PAA is proposed as shown in Fig.2(b). For comparison, a square PAA is shown in Fig.2(a). IRFPA fill factor $f$ is defined as the ratio of the PAA area to the pixel area, both horizontal and vertical pixel pitches are $p$ for both pixels. For simplicity, the "Z" shape is centrosymmetric and staggers along one-dimension (1D, horizontal axis). The upper half of the PAA is slightly shifted towards right, and the lower half of the PAA is equally shifted towards left. We define $k$ as the shape factor to describe the "Z" shape. $kp$ is the interval between the right boundary of the pixel and right side of the lower half PAA. Specific parameters are all indicated in Fig. 2.

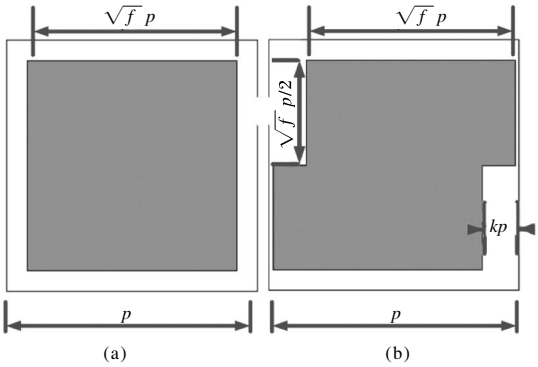


Fig. 2 (a) Square PAA model, (b) "Z" shape PAA model

Regardless of the PAA shapes, the normalized function of one pixel can be expressed as follow,

$$P(x,y)=\begin{cases}1/fp^2 & \text{for}(x,y)\text{ inside PAA}\\ 0 & \text{for}(x,y)\text{ outside PAA}\end{cases} \quad (1)$$

After doing Fourier-transforming with the two PAA shapes, we have,

$$MTF_{\text{Square}}(u,v)=f\,\text{sinc}(\pi uf^{1/2}p)\text{sinc}(\pi vf^{1/2}p) \quad (2)$$

$$MTF_{\text{"Z" shape}}(u,v)=f\,\text{sinc}(\pi uf^{1/2}p)\text{sinc}(\pi vf^{1/2}p)\times$$

$$\cos[\pi u(f^{1/2}+2k-1)p-\pi v f^{1/2}p/2] \quad (3)$$

We simulate the MTF for the two PAA shapes. The IRFPA fill factor $f$=60%, pixel pitch $p$=35 μm, shape factor $k$=0.15 and the vertical spatial frequency $v$=1/(2$p$). The calculation results based on Eq.(2), and (3) are shown in Fig.3 to indicate the MTF as a function of the horizontal spatial frequency $u$ for square PAA and "Z" shape PAA. In Fig. 3, we note that the difference between the MTFs of the "Z" shape PAA and the square PAA is large, for example, the MTFs of the "Z" shape PAA are respectively 71% at 50 lp/mm and 57% at 150 lp/mm of the MTFs of the square PAA. Both PAAs have the same fill factor $f$, so shape is the only reason causing this difference in MTF.

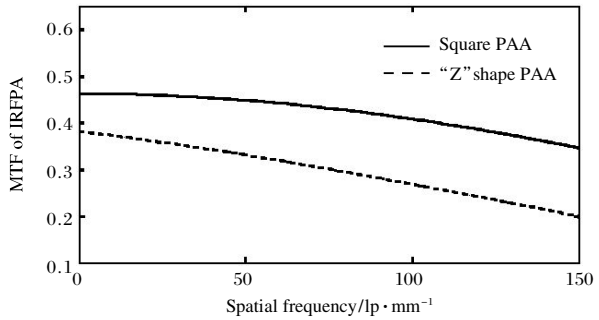


Fig. 3 MTFs of square PAA and "Z" shape PAA

We simulate the MTFs for different shape factor $k$ in "Z" shape PAA. The IRFPA fill factor $f$=60%, pixel pitch $p$=35 μm, the horizontal spatial frequency $u$=1/(2$p$) and the vertical spatial frequency $v$=0. The calculation results based on Eq. (3) are shown in Fig.4 to indicate the MTF as a function of the "Z" shape PAA shape factor $k$. When FPA fill factor $f$=60%, the interval of the shape factor is $0 \leqslant k \leqslant 0.22$. In Fig.4, the MTF is improved when $k$ becomes larger from 0 to 0.11, then degraded when $k$ varies from 0.11 to 0.22. When $k$=0.11, i.e. the "Z" shape PAA becomes a square, the MTF gets its peak value and reaches the MTF of the square PAA (dash line in Fig. 4).

From the calculation, we note that with the same fill factor $f$, different PAA shapes affect the MTF greatly, and in "Z" shape, the closer both half PAAs are to the vertical axis of the pixel, the higher the MTF will be. Furthermore, it is reasonable to propose a hypothesis that under the same fill factor, the closer the PAA boundaries are to the pixel center, the greater the MTF of IRFPA will be.

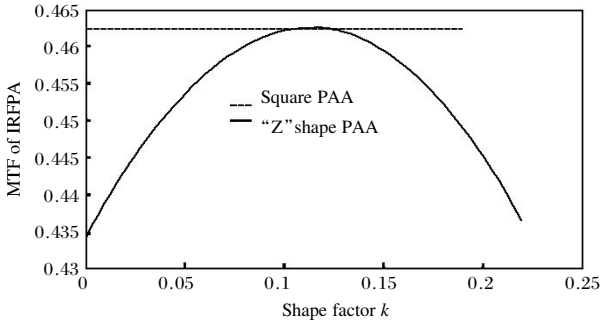


Fig.4 MTF of "Z" shape PAA as a function of shape factor $k$

## 2 PAA optimization for MTF of IRFPA

To describe how close the PAA boundaries are to the pixel center, we define centripetal index $i$ as follow,

$$i=\mathrm{Min}(|\mathrm{cir}(\vec{r})-\vec{o}|)/\mathrm{Max}(|\mathrm{cir}(\vec{r})-\vec{o}|) \quad (4)$$

where $\mathrm{cir}(\vec{r})$ is the function describes the PAA boundaries, $\vec{o}$ is the pixel center, $|\mathrm{cir}(\vec{r})-\vec{o}|$ is the distance between the pixel center and a certain point on PAA boundaries.

For simplicity, the PAA shapes to be discussed are limited in isogons. For an isogon with sides number $n$, the centripetal index $i$ is,

$$i=\cos(\pi/n) \quad (5)$$

It is obvious that $i$ achieves its maximum when $n=\infty$, i.e. the PAA shape is a circle.

In order to verify the hypothesis proposed in sec. 1, the IRFPA MTF of square ($n$=4, $i$=0.71), hexagon ($n$=6, $i$=0.87), octagon ($n$=8, $i$=0.92) and circle PAA ($n=\infty$, $i$=1) shapes (latter three shown in Fig.5, grey areas) will be discussed. Eq. (1) is still used as the normalized function of one pixel. Fourier-transforming with three different PAA shapes, we have Eq.(6), (7), and (8) for the MTFs of hexagon, octagon and circle PAA respectively. Eq.(6) and (7) are complex formulas.

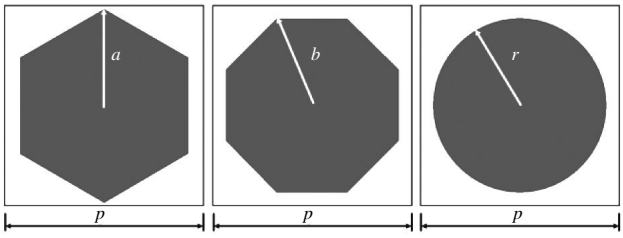


Fig.5 (a) Hexagon PAA, (b) Octagon PAA, (c) Circle PAA

$$MTF_{\mathrm{Hex}}(u,v)=f\frac{\sin(\frac{\sqrt{3}}{2}\pi a(-\frac{u}{\sqrt{3}}+v))}{\pi(-\frac{u}{\sqrt{3}}+v)\frac{3\sqrt{3}}{2}\pi a}\frac{\sin(2\pi ua+\frac{\sqrt{3}}{2}\pi a(-\frac{u}{\sqrt{3}}+v))}{\pi au}+f\frac{\sin(\frac{\sqrt{3}}{2}\pi a(\frac{u}{\sqrt{3}}+v))}{\pi(\frac{u}{\sqrt{3}}+v)\frac{3\sqrt{3}}{2}\pi a}\frac{\sin(2\pi ua-\frac{\sqrt{3}}{2}\pi a(\frac{u}{\sqrt{3}}+v))}{\pi au} \tag{6}$$

In Eq. (6), $a=\sqrt{2\sqrt{3}f}\,p/3$, a is the length of hexagon side.

$$\begin{aligned}MTF_{\mathrm{Oct}}(u,v)=&f\frac{\sin\left[(\frac{2-\sqrt{2}}{2}u-\frac{\sqrt{2}}{2}v)\pi b\right]}{\pi(u-\frac{\sqrt{2}}{2-\sqrt{2}}v)2\sqrt{2}\,b}\frac{\sin\left[(\frac{2-\sqrt{2}}{2-\sqrt{2}}\pi bv+(\frac{2+\sqrt{2}}{2}u-\frac{2+\sqrt{2}}{\sqrt{2}(2-\sqrt{2})}v)\pi b\right]}{\pi bv}+\\ &f\frac{\sin\left[(\frac{2-\sqrt{2}}{2}u+\frac{\sqrt{2}}{2}v)\pi b\right]}{\pi(u+\frac{\sqrt{2}}{2-\sqrt{2}}v)2\sqrt{2}\,b}\frac{\sin\left[(\frac{2\sqrt{2}}{2-\sqrt{2}}\pi bv+(\frac{2+\sqrt{2}}{2}u-\frac{2+\sqrt{2}}{\sqrt{2}(2-\sqrt{2})}v)\pi b\right]}{\pi bv}+\\ &f\frac{\sin\left[(\frac{2-\sqrt{2}}{2}u-\frac{\sqrt{2}}{2}u)\pi b\right]}{\pi(v-\frac{\sqrt{2}}{2-\sqrt{2}}u)2\sqrt{2}\,b}\frac{\sin\left[(\frac{2\sqrt{2}}{2-\sqrt{2}}\pi bu+(\frac{2+\sqrt{2}}{2}v-\frac{2+\sqrt{2}}{\sqrt{2}(2-\sqrt{2})}v)\pi b\right]}{\pi bu}+\\ &f\frac{\sin\left[(\frac{2-\sqrt{2}}{2}v+\frac{\sqrt{2}}{2}u)\pi b\right]}{\pi(v+\frac{\sqrt{2}}{2-\sqrt{2}}u)2\sqrt{2}\,b}\frac{\sin\left[(\frac{2\sqrt{2}}{2-\sqrt{2}}\pi bu-(\frac{2+\sqrt{2}}{2}v+\frac{2+\sqrt{2}}{\sqrt{2}(2-\sqrt{2})}u)\pi b\right]}{\pi bu}+\\ &f\frac{\sin(\sqrt{2}\,\pi bu)}{\sqrt{2}\,\pi bu}\frac{\sin(\sqrt{2}\,\pi bv)}{\sqrt{2}\,\pi bv}\end{aligned} \tag{7}$$

In Eq.(7), $b=\sqrt{\sqrt{2}f}\,p/2$, $b$ is the distance between octagon vertex and center.

$$MTF_{\mathrm{Circ}}(u,v)=r\,J_1(2r\pi\sqrt{u^2+v^2})/\sqrt{u^2+v^2} \tag{8}$$

In Eq.(8), $r=p\sqrt{f/\pi}$ , $r$ is the radius of circle, $J_1$ is the first order Bessel function of first kind.

The MTF for different PAA shapes is simulated. The IRFPA fill factor $f$=60%, pixel pitch $p$=35 μm, the vertical spatial frequency $v$=1/2$p$. The calculation results based on Eq.(2), (6), (7), and (8) are shown in Fig.6 to indicate the MTF as a function of the horizontal spatial frequency $u$ for different PAA shapes. We note that the MTF curve of circle PAA is the highest, followed by the MTF curve of octagon PAA and hexagon PAA, while the square PAA is the lowest. The calculation results are quite coincident with the hypothesis. Combining the hypothesis and the definition of the centripetal index $i$, we come to the conclusion that the smaller the difference between the closest and the farthest distances from the PAA boundaries to the pixel center, the greater the MTF of IRFPA will be.

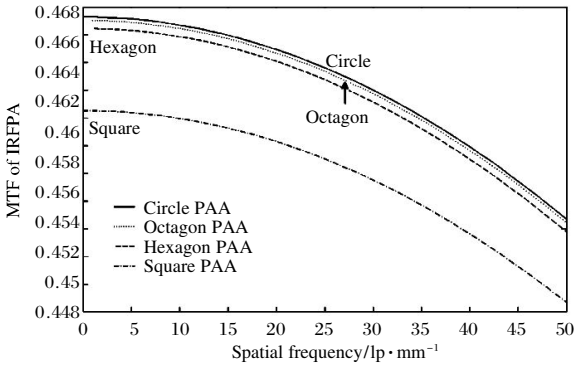


Fig.6 MTFs of square PAA, hexagon PAA, octagon PAA and circle PAA

Furthermore, the calculation results based on Eq.(2) and (8) are shown in Fig.7 to indicate the MTF difference between square PAA and circle PAA as a function of the IRFPA fill factor *f*. The difference becomes larger when the fill factor increases. Practically, the circle PAA radius *r* cannot be larger than half of pixel pitch *p*, in which case the fill factor *f*=0.78 (the vertical dash line in Fig. 7).

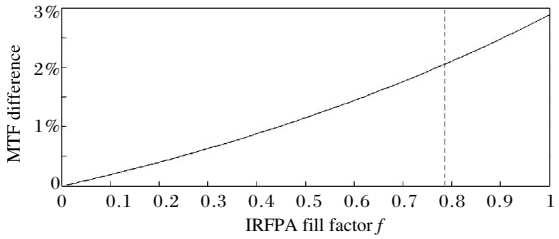


Fig.7 MTF difference (between circle and square PAA) as a function of IRFPA fill factor *f*

## 3 Conclusions

The MTF of different PAA shapes is discussed. The square PAA is currently widely used in research of MS for IR SR imaging, the "Z" shape PAA is proposed to simulate practical IRFPA production (GW20020131A GWIC Inc. China). The MTFs of these PAAs are obtained. Calculation results show that under the same fill factor, the difference of MTFs between the ideal square PAA and the "Z" shape PAA is large. The difference is caused only by the PAA shape, and under the same fill factor, the closer the PAA boundaries are to the pixel center, the larger the MTF will be. The MTFs of hexagon, octagon and circle PAA are also obtained. Calculation results show that under the same fill factor, the MTF of the circle PAA is the largest while that of the square PAA is the smallest, which proves the hypothesis that under the same fill factor, the smaller the difference between the closest and the farthest distances from the PAA boundaries to the pixel center, the greater the MTF of IRFPA will be. It is quite clear that the circle PAA is the most ideal model which causes the least degeneration of image quality, and it should be used as a reference for IRFPA design.

**References:**

[1] J M Wiltse, J L Miller. Imagery improvements in staring infrared imagers by employing subpixel microscan [J]. ***Opt Eng***, 2005, 44(5): 056401.

[2] A Bergeron, L L Noc, B Tremblay, et al. Flexible 640 x 480 pixel infrared camera module for fast prototyping [C]// Proc SPIE, 2009, 7481: 74810L.

[3] L L Noc, D Dufour, M Terroux, et al. Towards a very high-resolution infrared camera core [C]//Proc SPIE, 2011, 8012: 80123P.

[4] R R Schultz, R L Stevenson. Extraction of high-resolution frames from video sequences [J]. ***IEEE Transactions on Imaging Processing***, 1996, 5(6): 996-1011.

[5] K M Hock. Effect of oversampling in pixel arrays [J]. ***Opt Eng***, 1995: 34(5): 1281-1288.

[6] J C Gillete, T M Stadtmiller, R C Hardie. Aliasing reduction in staring infrared imagers utilizing subpixel techniques [J]. ***Opt Eng***, 1995, 34(11): 3130-3137.

[7] O Hadar, G D Boreman. Oversampling requirements for pixelated-imager systems[J]. ***Opt Eng***, 1999, 38(5): 782-785.

[8] K Krapels, R Driggers, R Vollmerhausen, et al. Performance comparison of rectangular (four-point) and diagonal (two-point) dither in undersampled infrared focal plane array imagers[J]. ***App Opt***, 2011, 40(1): 71-84.

[9] J L Miller, J M Wiltse. Benefits of microscan for staring infrared imagers[C]//Proc SPIE, 2004, 5407: 127-138.

[10] Z Wang, C E Glazowski, J M Zavislan. Modulation transfer function measurement of scanning reflectance microscopes [J]. ***J Bio Opt***, 2007, 12(5): 051802.

[11] X Wang, J Zhang, H Chang. The effect of fill factor of infrared FPA sensor on microscanning imagery quality [C]// Proc SPIE, 2005, 5640: 417-424.

[12] X Wang, H Hua. Theoretical analysis for integral imaging performance based on microscanning of a microlens array [J]. ***Opt Lett***, 2008, 33(5): 449-451.

[13] Y Li, F Lilley, D Burton, et al. Evaluation and benchmarking of a pixel-shifting camera for superresolution lensless digital holography[J]. ***App Opt***, 2010, 49(9): 1643-1650.

[14] X Sui, L Bai, Q Chen, et al. Influencing factors of microscanning performance based on flat optical component [J]. ***Chin Opt Lett***, 2011, 9(5): 052302.